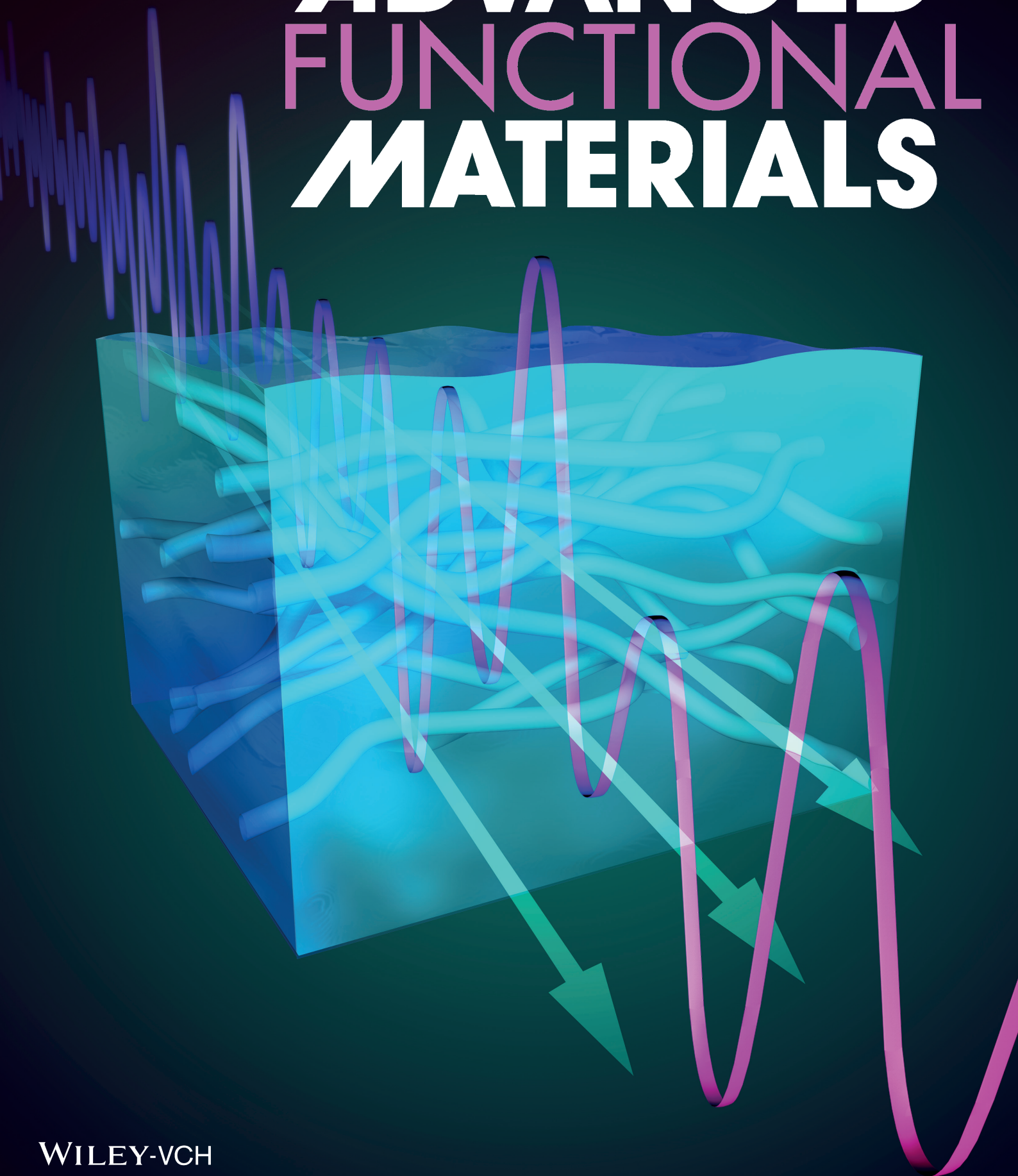# ADVANCED
FUNCTIONAL
MATERIALS

Metagel with Broadband Tunable Acoustic Properties Over Air–Water–Solid Ranges

Kai Zhang, Chu Ma, Qi He, Shaoting Lin, Yi Chen, Yu Zhang, Nicholas X. Fang,* and Xuanhe Zhao*

Materials capable of varying their acoustic impedances to match those of air, water, and solid materials over broadband frequencies will enable new applications in fields as diverse as medical imaging, underwater sonar and communication, and marine biology. However, such tunability has not been achieved with conventional acoustic materials including metals, polymers, ceramics and woods. Here, the invention of metagel, a class of designed hydrogel composites with unprecedented tunable acoustic properties over broadband frequencies, is reported. The metagel consists of patterned channels in a tough hydrogel matrix, where air, water, or liquid metal can be purged through the channels to tune the metagel's acoustic transmission over air–water–solid ranges and broadband frequencies on demand. It is shown that the acoustic properties of the metagel can be tuned by varying the volume ratio of the channels, properties, different filler materials with combined experiments, theory, and simulations. The metagel enables novel functions such as adjustable imaging regions of ultrasound, demonstrating tangible applications in underwater acoustics and medical imaging.

1. Introduction

Acoustic materials have attracted great research interests in recent years, exemplified by novel devices such as acoustic lenses,[1–6] cloaks,[7–9] and absorbers[10,11] with broad applications in medical imaging,[12–14] underwater sonar and communication, and marine biology.[15] Whereas conventional acoustic materials including metals, polymers, ceramics and woods are frequently used in various environments of solids, liquids and gases in different ranges of frequency, they cannot significantly change their acoustic properties once fabricated. Acoustic impedance mismatch between the acoustic materials and the environments causes energy loss and pulse aliasing, posing a grand challenge to acoustic imaging and communication. Addressing this challenge requires acoustic materials capable of varying acoustic impedance according to the different surrounding media and working frequencies. In particular, increasing resolution and efficiency of signal transductions in underwater and biomedical applications requires acoustic impedance match between the acoustic materials and water over broadband frequency. Previous works show that the acoustic impedance can be tailored by using metamaterial composites consisting of inclusions embedded in fluid. For example, the perfect matching of impedance with water is achieved in simulation for a variety of elastic shells embedded in water.[4] Inclusions of aerogel and solid cylinders embedded in air is also proposed to produce a perfect matching of impedance with that of air.[2] However, the acoustic properties of the structures in those works are still fixed and cannot provide real-time adjustment. Whereas mechanisms such as electro/magnetomechanical coupling[16–19] and structural deformation[20,21] have been employed to tune acoustic properties of solid materials, the ranges of tunable acoustic properties and frequencies are limited. To the best of our knowledge, there has been no report on acoustic materials capable of tuning acoustic properties with time, to match those of water, air and a variety of solid materials over broadband frequencies.

Here we propose metagel, a new approach and material system to achieve tunable acoustic properties over air–water–solid ranges and broadband frequencies based on a hydrogel matrix with designed channels that can be filled with various media. Since the major constituent of hydrogels is water (e.g., over 90 vol%), the density of and speed of sound in hydrogels are almost identical to the corresponding properties of water. Therefore, the acoustic impedance of hydrogels matches that

Dr. K. Zhang, Dr. Y. Chen
School of Aerospace Engineering
Beijing Institute of Technology
Beijing 100081, China
Dr. K. Zhang, Q. He, S. Lin, Dr. X. Zhao
Soft Active Materials Laboratory
Department of Mechanical Engineering
Massachusetts Institute of Technology
Cambridge, MA 02139, USA
E-mail: zhaox@mit.edu
Dr. C. Ma, Dr. Y. Zhang, Dr. N. X. Fang
Nanophotonics and 3D Nanomanufacturing Laboratory
Department of Mechanical Engineering
Massachusetts Institute of Technology
Cambridge, MA 02139, USA
E-mail: nicfang@mit.edu
Dr. X. Zhao
Department of Civil and Environmental Engineering
Massachusetts Institute of Technology
Cambridge, MA 02139, USA

The ORCID identification number(s) for the author(s) of this article can be found under https://doi.org/10.1002/adfm.201903699.
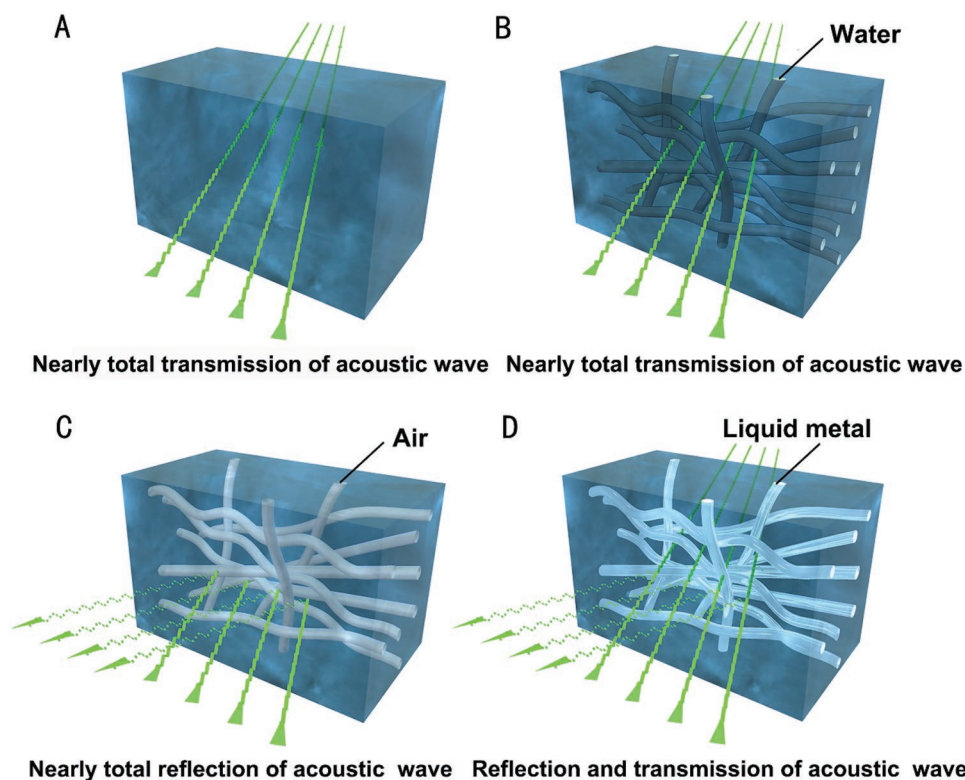
Figure 1. Schematics on the design of metagel consisting of microstructural channels in a tough hydrogel matrix. A) Acoustic impedance of the homogeneous hydrogel matches well with water, resulting in nearly total transmission of underwater acoustic wave. The effective acoustic properties of the microstructured metagel can be tailored by filling the channels with various liquids including B) water, C) air, and D) liquid metal, giving nearly total transmission, nearly total reflection and combined transmission and reflection of acoustic waves, respectively.

of water much better than any conventional acoustic material.[22] Meanwhile, the polymer networks in hydrogels endow them with elasticity, which maintains the shapes of hydrogel matrix and filler media in the matrix. In addition, hydrogels have been designed to be mechanically tough,[23,24] and tough hydrogels with microstructural features such as channels and cavities have been fabricated to give functional structures and devices.[22] A combination of the above-mentioned hydrogels' unique properties enables the design of metagel capable of unprecedented tunable acoustic properties.

2. Results

In **Figure 1**a, we schematically illustrate the design of metagel. The metagel is based on a tough hydrogel matrix, which achieves high toughness by integrating mechanisms for dissipating mechanical energy and maintaining high stretchability of polymer networks[25] (see the Experimental Section for details on tough hydrogel matrix). Since the acoustic impedance of the hydrogel well matches that of water,[22] underwater acoustic waves of various frequencies can achieve nearly complete transmission through the hydrogel matrix[22] (Figure 1a). Next, we design and fabricate a pattern of air channels with significant volume fraction in the tough hydrogel matrix and then connect the channels with a set of pumps. The pumps can purge various filler media including air, water and liquid metal

into the channels on demand (Figure 1a,b). We propose the following hypotheses for the design and operation of metagel. i) When the channels are filled with water, the metagel recovers the acoustic properties of water, resulting in the total transmission of acoustic wave. ii) When the channels are filled with air, the acoustic properties of metagel can approximate those of air, resulting in the total reflection of acoustic wave. iii) When the channels are filled with liquid metal, the acoustic properties of metagel can approach those of soft solid materials such as biological tissues and engineering rubbers, resulting in the combined transmission and reflection of acoustic waves. iv) The tunability is broadband.

To validate the above hypotheses, we adopt a pattern of equally spaced parallel channels in a tough hydrogel sheet, as shown in **Figure 2** (see the Experimental Section for details on fabrication of the hydrogel matrix with channels). The dimensions of the metagel sheet are 195 mm × 205 mm × 15.5 mm (length × width × thickness) with 31 circular channels embedded on the middle plane of the thickness direction and periodically arranged along the length direction. The diameter of the channel (a) is 2.2 mm, the distance between two adjacent channels (L) is 6.5 mm, and the length of the channel is 195 mm. A set of pumps are used to supply filler media including air, water and liquid metal (99.99% pure Gallium, The Gallium Shop) into the channels (Figure 2c). Figure 2 shows metagel sheet filled with water, air, and liquid metal. Another thinner metagel sheet, whose dimensions are 280 mm × 110 mm ×

**ADVANCED
SCIENCE NEWS**

www.advancedsciencenews.com

**ADVANCED
FUNCTIONAL
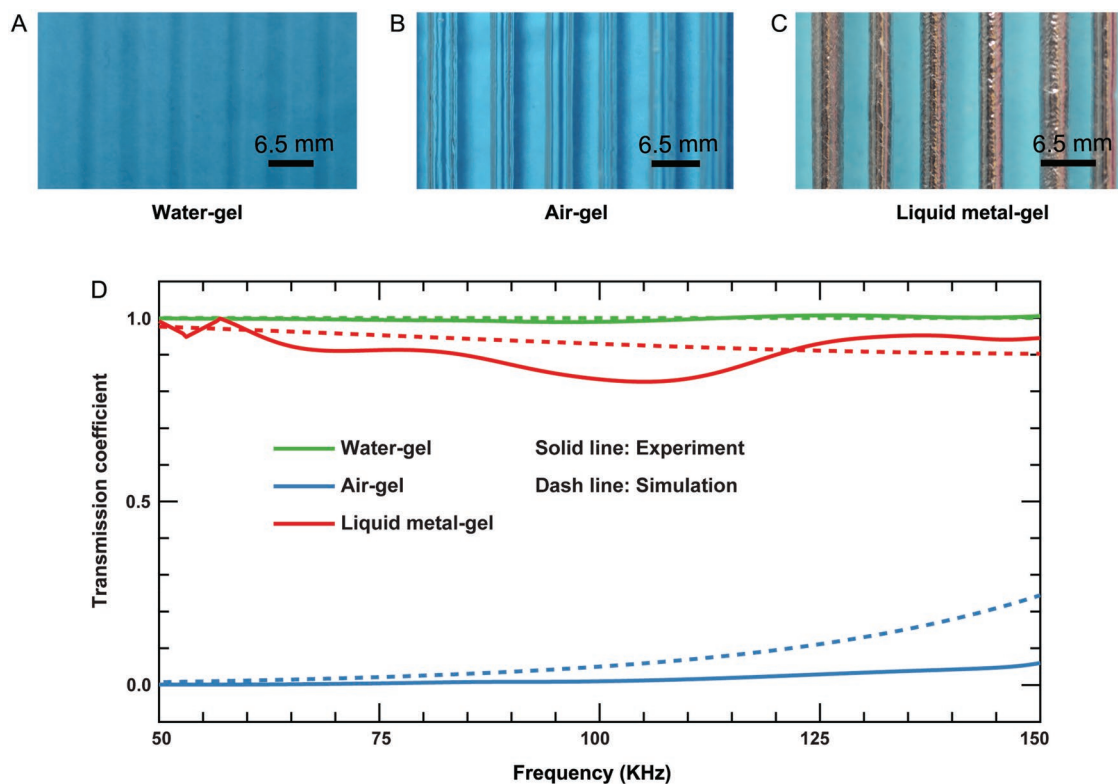MATERIALS**

www.afm-journal.de

Figure 2. Broadband tunable acoustic transmission through the metagel by changing filler materials. The images of the underwater metagel filled with water A), air B), and liquid metal C). D) Transmission coefficient of the metagel filled with water, air and liquid metal over various frequencies from experiment and numerical simulation. Solid lines represent experiment result while dash lines represent simulation result. The diameter of the channel is a = 2.2 mm and the distance between two adjacent channels is L = 6.5 mm.

6 mm (length × width × thickness) with 46 square channels, is also fabricated. The width of the square channel (a) is 3 mm, and the distance between two adjacent channels (L) is 6 mm. The corresponding images of this thinner metagel sheet filled with water, air, and liquid metal are shown in the Supporting Information. Movies S1–S3 (Supporting Information) demonstrate the process of pumping different filler media.

The sound transmission through the metagel sheet (195 mm × 205 mm × 15.5 mm) is measured in a water tank for frequencies from 50 to 150 kHz, a typical range for underwater acoustics, such as fish finding sonar, echo sounder, etc. (see the Supporting Information for details on experimental acoustic transmission coefficient measurements). Besides the structural design, we mainly propose to tune the acoustic properties of the metagel with two methods: 1) change filler materials inside the channels and 2) change the filling ratios of different materials.

3. First Tuning Method: Change Filler Materials

For the first method, we fill all the channels with one type of material (air, water, or liquid metal), and tune the acoustic properties by switching between different filler materials. The sound transmission through the metagel sheet is measured from 50 to 150 kHz. As shown in Figure 2d, the measured transmission coefficient of metagel sheet with water is above 0.989 in the frequency range from 50 to 150 kHz, indicating almost perfect

acoustic impedance match between the metagel and water. In contrast, when the channels in metagel sheet are filled with air, the transmission coefficient of metagel sheet reduces below 0.06 for all tested frequencies, giving nearly total refection of underwater acoustic waves. When the channels in metagel sheet are filled with liquid metal, the average transmission coefficient of metagel sheet is measured to be around 0.9. These results demonstrate that the metagel possesses tunable transmission coefficient of underwater acoustic waves in the frequency range of 50 to 150 kHz, by simply varying the filler materials.

4. Second Tuning Method: Change the Filling Ratios

In the second tuning method, we change the filling ratio of channels occupied by water and air while fixing the value of a and L. Here the diameter of the channel a is 2.2 mm and the distance between two adjacent channels L is 6.5 mm. N_{water} (N_{air}) denote the number of channels filled with water (air). **Figure 3**a–c shows the images of metagel sheets with different filling ratios. In Figure 3d, we plot the experimentally measured acoustic transmission coefficient with $N_{water}:N_{air}$ = 1:0, 1:3, 1:5, 1:8, 2:1, 2:2, 2:3, and 0:1, respectively, in frequency range from 50 to 150 kHz. By tuning N_{water} and N_{air}, the transmission coefficient can be tuned to cover the range from 0 to 1. The numerical simulated transmission coefficients for the same set of N_{water} and N_{air} are plotted Figure 3e (see the Supporting Information for

ADVANCED
SCIENCE NEWS
www.advancedsciencenews.com

ADVANCED
FUNCTIONAL
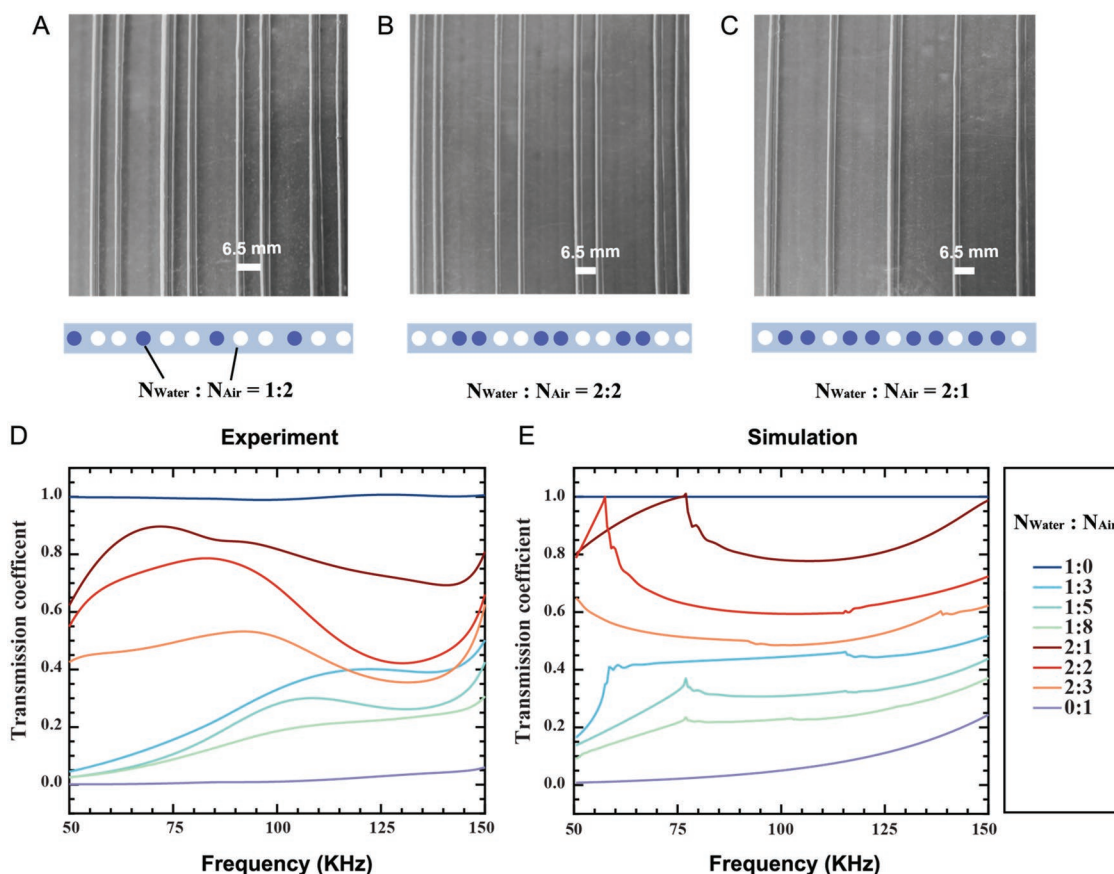**MATERIALS**
www.afm-journal.de

Figure 3. Broadband and wide-range tunable acoustic transmission of the metagel by changing the filling ratios. The images of the underwater metagel with different filling ratio. The ratio of water to air (N_{water}:N_{air}) can be mixed at A) 1:2, B) 2:2, and C) 2:1. D,E) Experiment and numerical transmission coefficients for the set of N_{water} and N_{air}. The width of the square channel $a = 2.2$ mm and the distance between two adjacent channels $L = 6.5$ mm.

details), showing similar trends as Figure 3d. The discrepancy between the experiment and the numerical simulation is mainly caused by the following factors: The experiment measures a finite system with boundaries while the simulation models an infinite periodic system. The viscous loss and background noise in experiments are not presented in the simulation.

To facilitate the design of tunable metagel based on the volume ratio of the channels, filler media and the filling ratio, we calculate the underwater acoustic transmission of the metagel sheet using multiple scattering theory (MST). Based on MST model, the acoustic transmission coefficient T of metagel sheet (Figure 2) can be calculated as

$$T = \left| 1 + \frac{2}{kL} \sum_{n=-\infty}^{n=+\infty} B_n \right|^2 \qquad (1)$$

where $k = \omega/c$ is the wave number of acoustic wave in water with ω the angular frequency and c is the speed of sound in water, and L is the distance between the neighboring channels in the MST model as shown in Figure S2 (Supporting Information). B_n are a series of functions that satisfy Equation (S16) in the Supporting Information. In the MST model, the acoustic velocity and density of water are taken as 1466 m s^{-1} and 1000 kg m^{-3}, respectively. Since the shear modulus of hydrogel is much lower than its bulk modulus, the hydrogel is regarded as a liquid with the

same acoustic velocity and density as water. The air is modeled as a non-dissipative medium with acoustic velocity 343 m s^{-1} and density 1.204 kg m^{-3}, respectively (see the Supporting Information for details). The velocity and density of the liquid metal are taken as 2847 m s^{-1} and 6250 kg m^{-3}, respectively.[26]

Using MST, we calculate the acoustic transmission coefficient over a wide frequency range of 0.4 kHz to 5 MHz (Figure S5, Supporting Information), showing the consistency with numerical simulation. According to the MST model, when the channels are filled with water, the transmission coefficient of metagel still maintains almost 1 from 0.4 kHz to 5 MHz, which also has been proved by experimental test and previous work.[22] By changing the filling ratio N_{air} and N_{water}, transmission coefficient in the range from 0 to 1 can be achieved from 0.4 to 150 kHz, beyond the range in experimental measurements. In addition, as increasing frequency range, acoustic transmission coefficient of the metagel gradually approaches to almost constant over MHz. Besides the MST model, the wave transmission behavior in this high frequency range can also be explained by the principle of geometrical acoustics.[27] The number of acoustic rays transmitted through the metagel layer is proportional to the projected area of the metagel regions that are impedance matched with water (i.e., the hydrogel part) on a plane perpendicular to the acoustic rays. The lowest acoustic transmission coefficient of air-gel sheet that can be achieved by
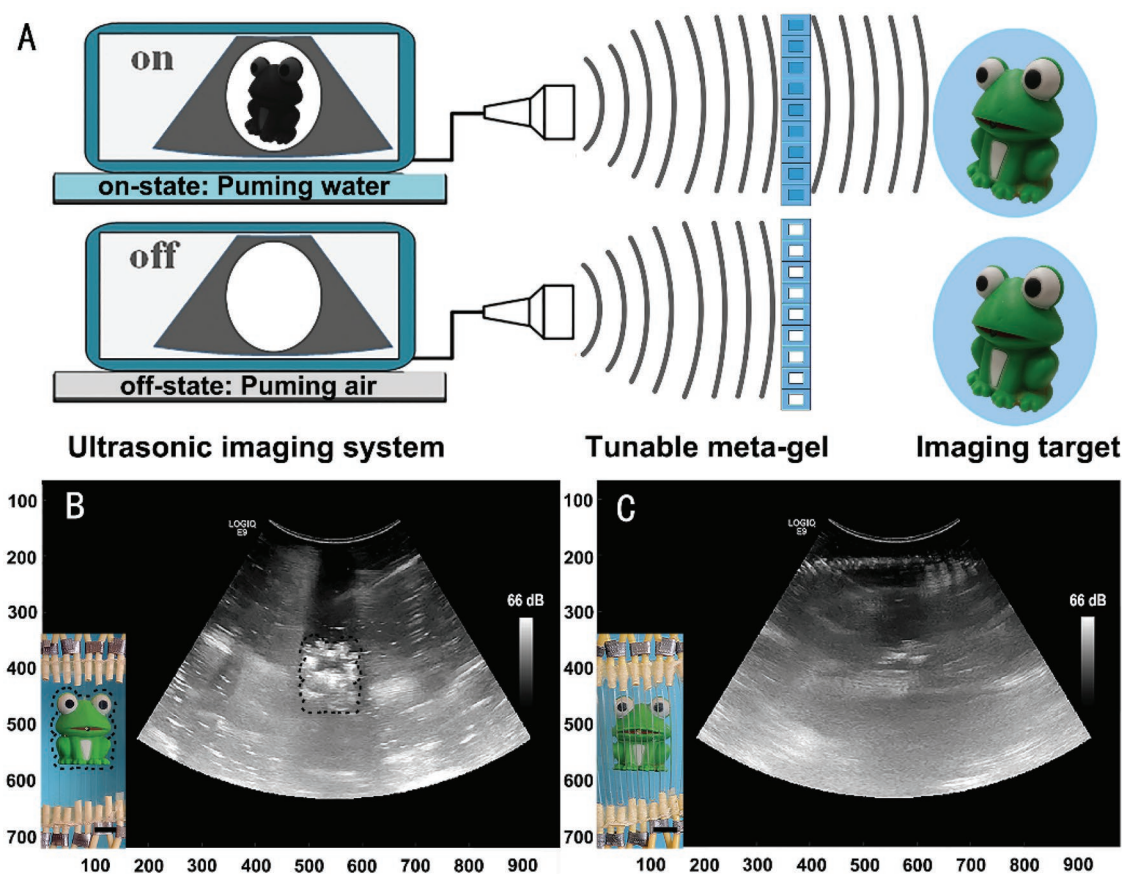
Figure 4. Application of the metagel in on-demand ultrasound imaging. A) Schematics of the on-demand ultrasound imaging system enabled by a metagel filled with water or air. Experimental results of ultrasound imaging through the metagel filled with B) water and C) air at 4 MHz. The target can be imaged clearly by ultrasound through a layer of metagel filled with water, while disappears once the channels in the metagel are filled with air. The scale bar of the optical image in (B) and (C) is 12 mm. The gray scale bar of the ultrasound image in (B) and (C) represents the dynamic range defined as the difference between the maximum and minimum values of the displayed signal.

the currently fabricated metagel sample with $a = 2.2$ mm and $L = 6.5$ mm is around 0.68. The area fraction of air-to-water for the fabricated metagel is 2.2:4.3. The acoustic transmission through the metagel is $4.3/(2.2 + 4.3) = 0.66$, which matches with the MST model and numerical simulation. The transmission coefficient increases linearly with the increase of L (i.e., the decrease of air's volume fraction). Thus, tunable transmission coefficient fully covering the range from 0 to 1 in high frequency can be achieved by designing air's volume fraction.

The tunable acoustic properties of the metagel at MHz frequency are also investigated by ultrasound imaging. As illustrated in **Figure 4**, a layer of the metagel is placed between the probe of an ultrasonic imaging system (GE LOGIQ E9; GE Healthcare) and a plastic frog all immersed in water. At frequency of 4 MHz, the frog can be clearly imaged by the ultrasound probe when the channels in the metagel are filled with water, but disappears once the channels are filled with air, as shown in 4b,c (Supporting Information). The horizontal lines of white spots in the upper part of the scan (Figure S4c, Supporting Information) are the air-gel sheet. Although the transmission coefficient of our used metagel sheet at MHz frequency is not zero, the metagel can still be used as a shutter for ultrasonic imaging with adjustable imaging windows. It is

indicated that acoustic wave can transmit through the metagel filled with water, but scattered by the metagel filled with air, where both the amplitude and phase of the acoustic wave are disturbed. We can achieve imaging windows of target objects with "on" state and "off" state on demand. The switch between the "on" state and the "off" state is controlled by pumping water or air into the corresponding regions of the metagel. This capability of selectively blocking unwanted region of strong scattering can potentially enable ultrasound imaging with enhanced contrast.

If the acoustic wavelength is larger than microstructural features of a metagel (e.g., channel diameter), the metagel can be taken as a macroscopically homogeneous material. The effective material properties are calculated with effective medium theory.[28] With the effective parameter retrieval method,[28] we calculate the acoustic impedance of the metagel with all the channels filled with water, air, or liquid metal, from the transmission and reflection coefficients from numerical simulation in COMSOL (see the Supporting Information for details on the calculation). The acoustic impedance of the metagel as a homogenous material can be expressed as[29] $Z = \sqrt{\rho_{\text{eff}} \cdot K_{\text{eff}}}$, where ρ_{eff} and K_{eff} are the effective density and bulk modulus of the metagel, respectively. The values of ρ_{eff} and K_{eff}

ADVANCED
SCIENCE NEWS
www.advancedsciencenews.com

ADVANCED
FUNCTIONAL
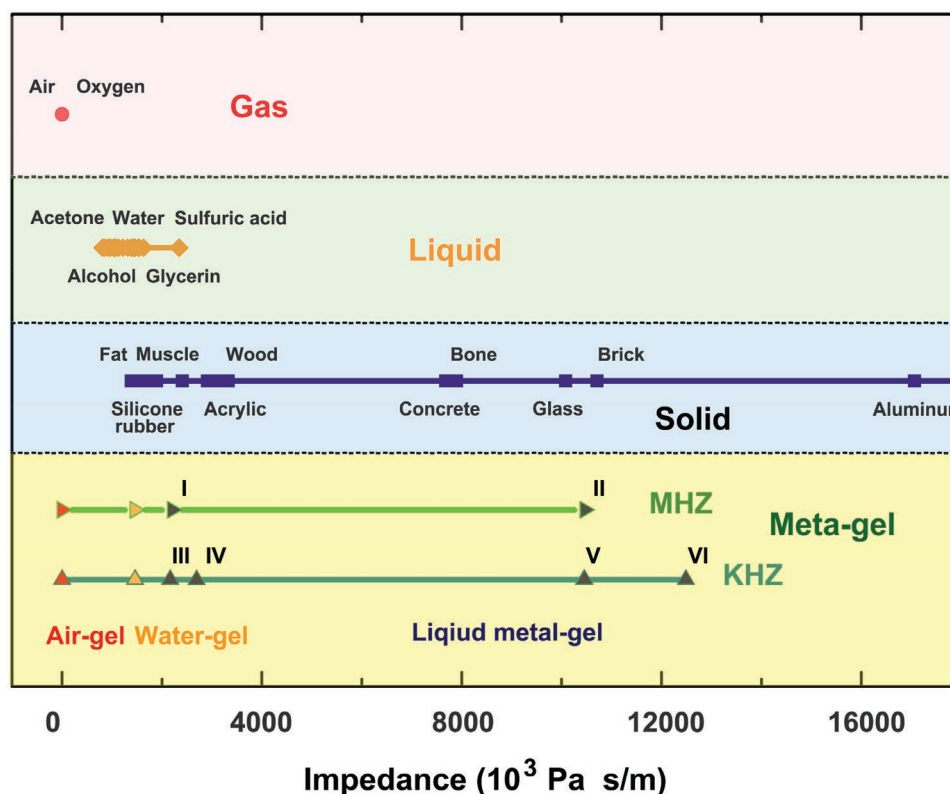**MATERIALS**
www.afm-journal.de

Figure 5. Acoustic impedances for various types of solids, liquids and gases in comparison with the metagel filled with various ratios of fillers and different dimensions. Metagel sheet with six different structural feature are proposed. I: $a = 110$ µm, $L = 325$ µm; II: $a = 110$ µm, $L = 115$ µm; III: $a = 2.2$ mm, $L = 6.5$ mm, used in experiments; IV: $a = 3$ mm, $L = 6$ mm; V: $a = 2.2$ mm, $L = 2.3$ mm; VI: $a = 3$ mm, $L = 3.1$ mm.

depend on the density and bulk modulus of the filler media. In comparison, we further give the Z values of typical gases, liquids and solids.

We plot the Z values of metagel with different dimensions and filler ratios in **Figure 5**. Z values of all the air-gel sheet occupies the region where acoustic impedance is close to zero. The Z values of all the water-gel sheets keep the same as water, which is independent on the structural feature, while that of liquid metal-gel sheets vary with increasing filling volume fraction (data points I–VI). By tuning the filler media, the metagel sheet with the channel pattern used in experiments (i.e., $a = 2.2$ mm, $L = 6.5$ mm) can possess a region of Z between 3.75×10^3 and 2.16×10^6 Pa s m^{-1}. The metagel sheet with $a = 3$ mm, $L = 6$ mm have a larger region of Z between 0.18×10^3 and 2.70×10^6 Pa s m^{-1}, which almost covers the Z values of typical liquids (e.g., water, acetone, benzene, ethyl alcohol, carbon tetrachloride, glycerin, oil, toluene, seawater, and sulfuric acid, in the range of 0.81×10^6 to 2.34×10^6 Pa s m^{-1}) and soft solids (e.g., fat, muscle, blood, rubber, polyethylene, polystyrene, in the range of 1.39×10^6 to 2.41×10^6 Pa s m^{-1}), even approaching the Z values of gases (e.g., air, oxygen, nitrogen, argon, chloroform, in the range of 0.41×10^3 to 0.51×10^3 Pa s m^{-1}). To further expand the metagel's tunable range of Z, we choose other dimensions of the channel pattern (i.e., $a = 2.2$ mm, $L = 2.3$ mm, or $a = 3$ mm, $L = 3.1$ mm,), so that the channels occupy a higher volume fraction of the metagel sheet than the previous structure. Z of the metagel with $a = 2.2$ mm and $L = 2.3$ mm can

reach to 1.04×10^7 Pa s m^{-1} by filling liquid metal, while the liquid metal-gel with $a = 3$ mm and $L = 3.1$ mm can achieve the maximum value of Z to 1.25×10^7 Pa s m^{-1} (Figure 5). When the wavelengths of acoustic waves in water are larger than the feature sizes of metagel sheet, the tunability of Z is based on material composition instead of resonance, so the metagel works broadbandly. When the feature size of metagel sheet is shifted down to micro size (i.e., $a = 110$ µm, $L = 115$ µm), simulation shows that the working frequency range of tunable Z is shifted to MHz (Figure 5) (see the Supporting Information for details).

5. Conclusion

In this work, we use tough hydrogels with designed patterns of channels filled with air, water, or liquid metal to achieve tunable acoustic properties that match those of air, water and soft solids over broadband frequencies. Besides the unprecedented broadband tunable acoustic transmission, the proposed metagel is also low cost, environmentally friendly, and compatible with human body. The method and material system reported here open new avenues to both design and applications of future acoustic materials. For example, while parallel channels of millimeter size have been adopted in the current metagel sheet, more sophisticated 2D or 3D channel patterns with finer features may lead to better tunability and/or broader

range of acoustic properties. Other filler media such as silicone oil or glycerol may be explored for future metagels. The tunable impedance match of metagel with water and various soft solid materials over broadband frequencies will facilitate the development of new underwater acoustic devices and medical imaging devices.

6. Experimental Section

Hydrogel Materials: In the tough hydrogel, Acrylamide (AAm; Sigma-Aldrich A8887) was used as the monomer for the covalently crosslinked stretchy network and Sodium alginate (Sigma-Aldrich A2033) ionically was used for the physically crosslinked dissipative network. In the polyacrylamide (PAAm) network, *N,N*-methylenebisacrylamide (Bis; Sigma-Aldrich 146072) was used as crosslinker and ammonium persulphate (APS, Sigma A3678) was used as photoinitiator. Calcium chloride solution (Sigma 746495) was prepared for the tough hydrogel, to provide the calcium ion crosslinked with Sodium alginate.

Fabrication on Metagel Composite: The metagel sheet consisted of straight channels arranged in the tough hydrogel matrix. A mold with 46 detachable bars was first designed and fabricated using laser cutter (Epilog Mini/Helix; Epilog Laser) based on computer aided design drawings. Crosslinked hydrogels were fabricated by pouring pregel solution into the mold and covering glass plates. The pregel solution for the soft PAAm–alginate hydrogel was prepared by mixing carefully degassed aqueous solution (12 wt% AAm, 2 wt% sodium alginate, 0.2 wt% Bis, and 0.2 mol L^{-1} APS). The crosslinked hydrogels in the mold were kept in a humid chamber for one hour to make sure the formation of crosslinks. Thereafter, the crosslinked hydrogel sample was carefully separated from the mold. The hydrogel sample with channels were immersed in calcium chloride solution (2.22 wt%) for 4 days to generate the tough hydrogel, and then in deionized water at least for 4 days to reach equilibrium swollen state. Finally, the neighboring channels in the hydrogel were connected by using a latex tube and sealed with superglue.

Acoustic Measurement of the Transmission Coefficient of the Metagel Sheet: We conducted transmission measurements for the fabricated sample with a = 2.2 mm (channel diameter) and L = 6.5 mm (period). The whole sample has dimension of 195 mm × 205 mm × 15.5 mm with 31 channels. The emitter is held fixed at the bottom of the water tank, with a 10 cm perpendicular distance to the middle of the sample. The sample is held completely horizontal and stable on an acrylic plastic ring plate which is fixed by four rods extending from the top platform. The receiver is placed 2 cm above the sample, and it is attached to a 2D moving stage which is attached to the top platform.

For each configuration of the channel filling, we measure the acoustic transmission through the sample for frequency range [50, 150] kHz with CTG Model ITC-1042 (emitter) and CTG Model ITC-1089D (receiver). The emitter sends a pulse wave with the form $P_{in} = \cos(2\pi \times 5 \times 10^4 t)$, where $t \in [0, 1/(4 \times 10^5)]$ s. A receiver scans a region of 5 cm^2 located 2 cm above and parallel to the sample. At each scanning point, a transmitted signal is measured as a time domain waveform. A time window is multiplied to the measured signal to get the portion of direct transmitted signal through the sample and eliminate reflections and those transmitted through the surrounded opening in the water tank. We then perform Fourier transform to the time-windowed signal to obtain the frequency spectrum. The spectrum covers the frequency range of [50, 150] kHz. After getting the frequency spectrums for all the points in the scanning region, we compute the average power spectrum by averaging the square of each individual frequency spectrum. The transmission coefficient of each channel filling configuration is obtained from the ratio of two measurements. One measurement is performed when the sample is put in the water tank, and anther measurement is performed when sample removed, serving as reference.

Supporting Information

Acknowledgements

Conflict of Interest

The authors declare no conflict of interest.

Keywords

[1] E. Meyer, E. G. Neumann, *Physics and Applied Acoustics—An Introduction*, Academic Press, New York **1972**.
[2] D. Torrent, J. Sánchez-Dehesa, *New J. Phys.* **2007**, *9*, 323.
[3] T. P. Martin, M. Nicholas, G. J. Orris, L. W. Cai, D. Torrent, J. S´anchez-Dehesa, *Appl. Phys. Lett.* **2010**, *97*, 113503.
[4] T. P. Martin, C. N. Layman, K. M. Moore, G. J. Orris, *Phys. Rev. B* **2012**, *85*, 161103.
[5] N. Kaina, F. Lemoult, M. Fink, G. Lerosey, *Nature* **2015**, *525*, 77.
[6] X. Su, A. N. Norris, C. W. Cushing, M. R. Haberman, P. S. Wilson, *J. Acoust. Soc. Am.* **2017**, *141*, 4408.
[7] H. Chen, C. T. Chan, *Appl. Phys. Lett.* **2007**, *91*, 183518.
[8] B. I. Popa, L. Zigoneanu, S. A. Cummer, *Phys. Rev. Lett.* **2011**, *106*. 253901.
[9] S. Zhang, C. Xia, N. Fang, *Phys. Rev. Lett.* **2011**, *106*, 024301.
[10] D. Y. Maa, *J. Acoust. Soc. Am.* **1998**, *104*, 2861.
[11] A. Climente, D. Torrent, J. Sanchez-Dehesa, *Appl. Phys. Lett.* **2012**, *100*, 144103.
[12] C. Errico, J. Pierre, S. Pezet, Y. Desailly, Z. Lenkei, O. Couture, M. Tanter, *Nature* **2015**, *527*, 499.
[13] L. V. Wang, S. Hu, *Science* **2012**, *335*, 1458.
[14] K. Melde, A. G. Mark, T. Qiu, P. Fischer, *Nature* **2016**, *537*, 518.
[15] X. Lurton, *An Introduction to Underwater Acoustics: Principles and Applications*, Springer Science & Business Media, Heidelberg **2002**.
[16] L. Airoldi, M. Ruzzene, *New J. Phys.* **2011**, *13*, 113010.
[17] B. I. Popa, S. A. Cummer, *Nat. Commun.* **2014**, *5*, 3398.
[18] Z. Wang, Q. Zhang, K. Zhang, G. Hu, *Adv. Mater.* **2016**, *28*, 9857.
[19] F. Casadei, T. Delpero, A. Bergamini, P. Ermanni, M. Ruzzene, *J. Appl. Phys.* **2012**, *112*, 064902.
[20] P. Wang, F. Casadei, S. Shan, J. C. Weaver, K. Bertoldi, *Phys. Rev. Lett.* **2014**, *113*, 014301.
[21] S. Babaee, J. T. B. Overvelde, E. R. Chen, V. Tournat, K. Bertoldi, *Sci. Adv.* **2016**, *2*, e1601019.

[22] H. Yuk, S. Lin, C. Ma, M. Takaffoli, N. X. Fang, X. Zhao, *Nat. Commun.* **2017**, *8*, 14230.

[23] J. P. Gong, Y. Katsuyama, T. Kurokawa, Y. Osada, *Adv. Mater.* **2003**, *15*, 1155.

[24] J. Y. Sun, X. Zhao, W. R. K. Illeperuma, O. Chaudhuri, K. H. Oh, D. J. Mooney, J. J. Vlassak, Z. Suo, *Nature* **2012**, *489*, 133.

[25] X. Zhao, *Soft Matter.* **2014**, *10*, 672.

[26] S. Ayrinhac, M. Gauthier, G. L. Marchand, M. Morand, F. Bergame, F. Decremps, *J. Phys.: Condens. Matter* **2015**, *27*, 275103.

[27] M. J. Crocker, *Handbook of Acoustics*, John Wiley & Sons, New York **1998**.

[28] V. Fokin, M. Ambati, C. Sun, X. Zhang, *Phys. Rev. B* **2007**, *76*, 144302.

[29] D. Torrent, J. Sánchez-Dehesa, *Phys. Rev. B* **2006**, *74*, 224305.

**ADVANCED
FUNCTIONAL
MATERIALS**

Supporting Information

Metagel with Broadband Tunable Acoustic Properties Over Air–Water–Solid Ranges

Kai Zhang, Chu Ma, Qi He, Shaoting Lin, Yi Chen, Yu Zhang, Nicholas X. Fang,* and Xuanhe Zhao*

Supporting Information

Title Meta-gel with broadband tunable acoustic properties over air-water-solid ranges

Kai Zhang, Chu Ma, Qi He, Shaoting Lin, Yi Chen, Yu Zhang, Nicholas X. Fang*, Xuanhe Zhao*

This file includes:

Supporting Text

Figures. S1-S6

Tables S1-S3

Movies S1-S3

Acoustic measurement of the transmission coefficient of the meta-gel sheet

We conducted transmission measurements for the fabricated sample with a=2.2 mm (channel diameter) and L=6.5 mm (period). The whole sample has dimension of 195 mm × 205 mm × 15.5 mm with 31 channels. The emitter is held fixed at the bottom of the water tank, with a 10 cm perpendicular distance to the middle of the sample. The sample is held completely horizontal and stable on an acrylic plastic ring plate which is fixed by four rods extending from the top platform. The receiver is placed 2 cm above the sample, and it is attached to a 2D moving stage which is attached to the top platform.

For each configuration of the channel filling, we measure the acoustic transmission through the sample for frequency range [50, 150] KHz with CTG Model ITC-1042 (emitter) and CTG Model ITC-1089D (receiver). The emitter sends a pulse wave with the form $P_{in}=\cos(2\pi\times5\times10^4t)$, where $t\in$ $[0,1/(4\times10^5)]$ s. The time domain waveform and the Fourier spectrum of P_{in} are plotted in **Figure S1**a-b. A receiver scans a region of $5\ cm^2$ located 2 cm above and parallel to the sample. At each scanning point, a transmitted signal is measured as a time domain waveform. A typical measured signal P_{out} for frequency range [50, 150] KHz is plotted in **Figure S1**c. A time window is multiplied to the measured signal to get the portion of direct transmitted signal through the sample and eliminate reflections and those transmitted through the surrounded opening in the water tank. We then perform Fourier transform to the time-windowed signal to obtain the frequency spectrum (**Figure S1**d). The spectrum covers the frequency range of [50, 150] KHz. After getting the frequency spectrums for all the points in the scanning region, we compute the average power spectrum by averaging the square of each individual frequency spectrum. The transmission coefficient of each channel filling configuration is obtained from the ratio of two measurements. One measurement is performed when the sample is put in the water tank, and anther measurement is performed when sample removed, serving as reference. We plot the acoustic transmission coefficients for different filling configurations in frequency range [50, 150] KHz.
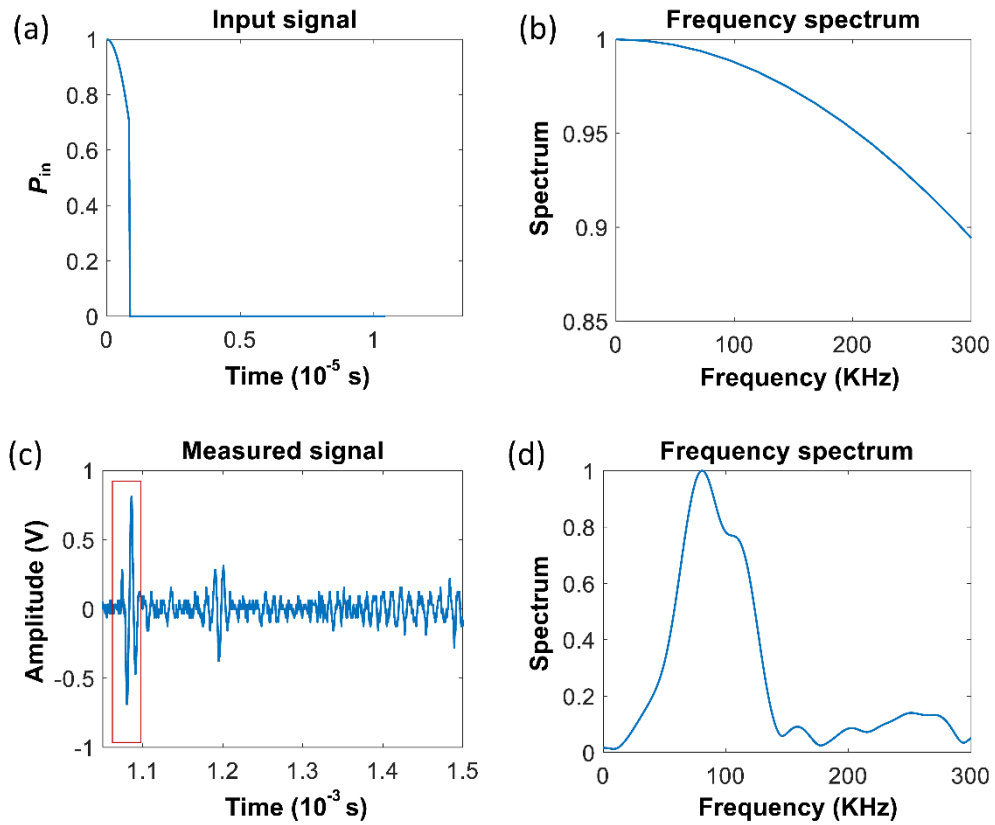
Figure S1 Measurements for [50, 150] KHz frequency range. **(a)** Time domain waveform of input signal. **(b)** Frequency spectrum of input signal. **(c)** An example of received signal. The region inside the red rectangle is the time windowed signal. **(d)** Frequency spectrum of time-windowed measured signal.

Multiple scattering theory (MST) for underwater acoustic transmission of the meta-gel sheet
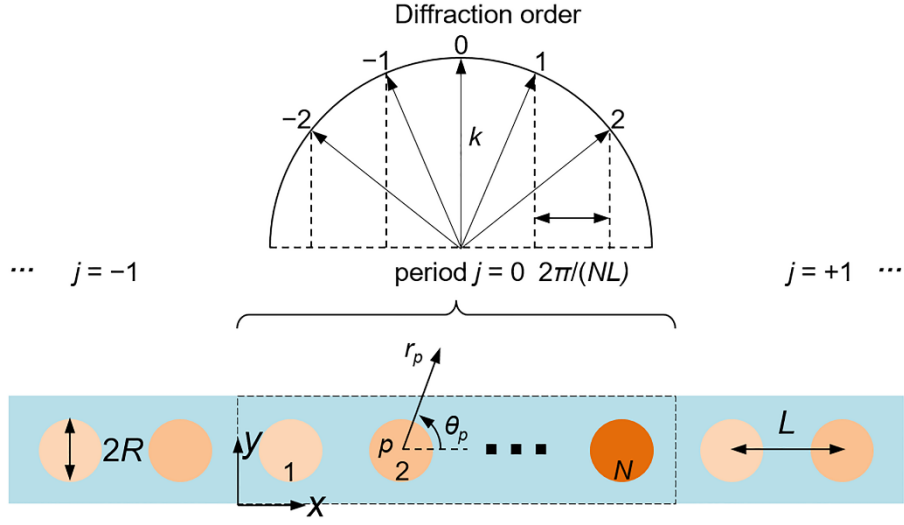

Figure S2. Scheme of acoustic scattering by a periodic lattice composed of N scatters.

This part derives the acoustic scattering solution for a one-dimensional periodic lattice (**Figure S2**). Each period is composed of N circular nonmental scatters with the same radius R and a distance L between neighboring channels. Here we use circular scatter filled with fluid materials. Numerical simulations have validated that a meta-gel with circular scatter of radius R give almost the same acoustic properties as otherwise the same meta-gel with square scatter of width $a = \sqrt{\pi}R$. The normally incident plane wave in the background fluid is,

$$p^{\mathrm{in}} = \exp(iky) \hspace{5cm} \text{S(1)}$$

k is the wave number in the background fluid. Scattered pressure for the pth scatter in the jth period is,

$$p_{j,p}^{\mathrm{sc}} = \sum_{n=-\infty}^{n=+\infty} B_n^{(j,p)} H_n(kr_{j,p}) \exp(in\theta_{j,p}) \hspace{3cm} \text{S(2)}$$

Here, $B_n^{(j,p)}$ is the nth order scattering coefficient, $(r_{j,p}, \theta_{j,p})$ are the polar coordinate with the origin located at the center of the pth scatter in the jth period. $H_n(x)$ represents the nth order Hankel function of the first kind. Under the normal incidence condition, scattering coefficients $B_n^{(j,p)}$ of the pth scatter in each period are the same,

$$B_n^{(j,p)} = B_n^{(0,p)} = B_n^p \tag{S(3)}$$

The totally scattered pressure in the background is composed of scattering pressure from each scatter,

$$p^{tot} = \sum_{q=1}^{N} \sum_{j=-\infty}^{j=+\infty} \sum_{m=-\infty}^{m=+\infty} B_m^q H_m(kr_{j,q}) \exp(im\theta_{j,q}) \tag{S(4)}$$

This scattered pressure can be described as a summation of plane waves of different diffraction orders,

$$p^{tot} = \sum_{n=-\infty}^{n=+\infty} P_n \exp(ik\cos\theta_n x + ik\sin\theta_n \,|\, y\,|), \quad \cos\theta_n = n\frac{2\pi}{kNL} \tag{S(5)}$$

$$P_n(y) = \frac{2}{kL\sin\theta_n} \sum_{q=1}^{N} \exp(-i\frac{2n\pi}{NL} R_{0,q}) \sum_{m=-\infty}^{m=+\infty} B_m^q (-i)^m \exp(im\,\mathrm{sgn}(y)\theta_n) \tag{S(6)}$$

Transmission coefficient and reflection coefficient are,

$$T_n = \delta_{0n} + \frac{2}{kL\sin\theta_n} \sum_{q=1}^{N} \exp(-i\frac{2n\pi}{NL} R_{0,q}) \sum_{m=-\infty}^{m=+\infty} B_m^q (-i)^m \exp(im\theta_n) \tag{S(7)}$$

$$R_n = \frac{2}{kL\sin\theta_n} \sum_{q=1}^{N} \exp(-i\frac{2n\pi}{NL} R_{0,q}) \sum_{m=-\infty}^{m=+\infty} B_m^q (-i)^m \exp(-im\theta_n) \tag{S(8)}$$

For, $n=0$,

5

$$T_0 = 1 + \frac{2}{ka} \sum_{n=-\infty}^{n=+\infty} B_n$$

$$R_0 = \frac{2}{ka} \sum_{n=-\infty}^{n=+\infty} (-1)^n B_n$$

S(9)

The energy transmission rate is,

$$T = \frac{E_T}{E_I} = \sum_{n=-M}^{n=+M} \sin\theta_n |T_n|^2, \quad M = [\frac{ka}{2\pi}]$$

S(10)

in which, $[x]$ represents the maximal integer smaller than x. M is assumed to be zero for frequency lower than 150 KHz in the manuscript.

In the following, we derive the scattering coefficient B_m^q. Using the Graf's addition theorem [S1], incident pressure on the pth scatter in the 0th period is composed of scattering from all other scatters,

$$p_{0,p}^{in} = \sum_{n=-\infty}^{n=+\infty} \left(1 + \sum_{q \neq p}^{N} \sum_{m=-\infty}^{m=+\infty} G_{m,n}^{p,q}(0)B_m^q + \sum_{q=1}^{N} \sum_{m=-\infty}^{m=+\infty} G_{m,n}^{p,q} B_m^q \right) J_n(kr_{0,p}) \exp(in\theta_{0,p})$$

S(11)

$J_n(x)$ represents the nth order Bessel function, and

$$G_{m,n}^{p,q} = \sum_{j=1}^{+\infty} (1 + (-1)^{m-n}) H_{m-n}(k | jL | + k \operatorname{sgn}(j)(R_{0,q} - R_{0,p}))$$

S(12)

$$G_{m,n}^{p,q}(0) = \gamma_{q-p} H_{m-n}(k | R_{0,q} - R_{0,p} |)$$

S(13)

$$\gamma_{q-p} = \begin{cases} (-1)^{q-p}, & q-p > 0 \\ 1, & q-p < 0 \end{cases}$$

S(14)

Here, $R_{0,q}$ and $R_{0,p}$ represents the location of the qth and p^{th} scatter in the 0th period. At the boundary ($r_p = R$) of the pth scatter in the 0th period, the following continuous conditions is,

6

$$\begin{cases} p_{0,p}^{\text{in}} + p_{0,p}^{\text{sc}} = \sum_{n=-\infty}^{n=+\infty} A_n J_n(k_p R) \\ \dfrac{\text{d}}{\text{d}r}(p_{0,p}^{\text{in}} + p_{0,p}^{\text{sc}}) = \dfrac{\rho_0}{\rho_p} \sum_{n=-\infty}^{n=+\infty} A_n J_n'(k_p R) \end{cases}$$

S(15)

Substitute above equations S(2) and S(11), then we have,

$$\sum_{q \neq p}^{N} \sum_{m=-\infty}^{m=+\infty} G_{m,n}^{p,q}(0) B_m^q + \sum_{q=1}^{N} \sum_{m=-\infty}^{m=+\infty} G_{m,n}^{p,q} B_m^q + B_n^p \frac{\eta}{\xi} = -1$$

S(16)

This equation is an infinite dimension linear matrix equation, and can be solved by introducing a cut off order n_0 for n and then the scattering coefficient B_m^q can be solved. The parameters are defined as,

$$\xi = \frac{J_n(N_p kR)}{J_n(kR)} - \frac{1}{N_p Z_p} \frac{J_n'(N_p kR)}{J_n'(kR)}$$

S(17)

$$\eta = \frac{J_n(N_p kR)}{J_n(kR)} \frac{H_n'(kR)}{J_n'(kR)} - \frac{1}{N_p Z_p} \frac{J_n'(N_p kR)}{J_n'(kR)} \frac{H_n(kR)}{J_n(kR)}$$

S(18)

$$\frac{c_0}{c_p} = N_p, \quad \frac{\rho_p c_p}{\rho_0 c_0} = Z_p$$

S(19)

(ρ_p and c_p) represents the density and sound velocity of the pth scatter.

Meta-gel sheet filled with water, air and liquid metal and acoustic field through the meta-gel sheet

We adopt a pattern of equally spaced parallel channels in a tough hydrogel sheet, as shown in **Figure S3**. The dimensions of the hydrogel sheet in **Figure S3** are 280 mm × 110 mm × 6 mm (length ×

width ×thickness) with 46 square channels embedded on the middle plane of the thickness direction
and periodically arranged along the length direction. The width of the square channel (a) is 3 mm,
the distance between two adjacent channels (L) is 6 mm, and the length of the channel is 110 mm.
The adjacent channels are then connected using latex tubes with diameter of 3 mm and sealed with
superglue. A set of pumps are used to supply filler media including air, water and liquid metal
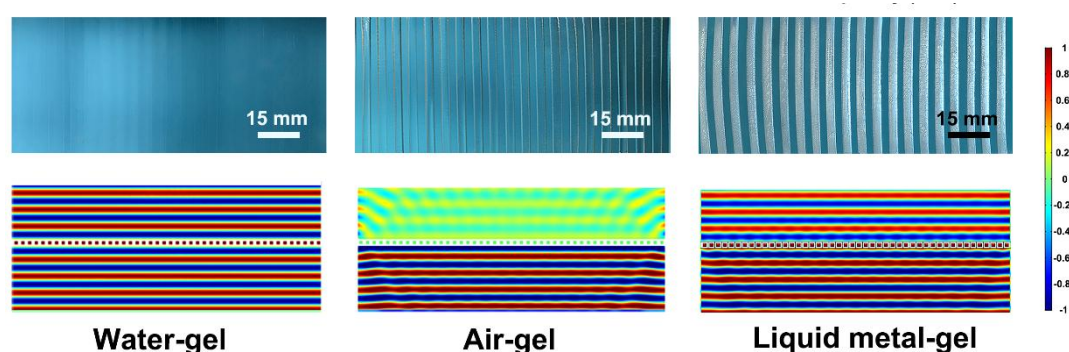(99.99% pure Gallium, The Gallium Shop) into the channels.

Figure S3. The images of the underwater meta-gel filled with water, air and liquid metal and the
contours of the acoustic field through the meta-gel sheet filled with water, air and liquid metal by
numerical simulation. The scale bar indicates the acoustic pressure normalized by incident pressure
amplitude.

COMSOL simulation on underwater acoustic transmission of the meta-gel. The underwater
acoustic transmission of the meta-gel was investigated in COMSOL Multiphysics based on the
multiple scattering decomposition method. For example, the simulation model for the channel filling
configuration water: air =1:2 was shown in **Figure S4**. The hydrogel was described by a nearly
incompressible Neo-Hookean material model, while the air and water were described by acoustic

8

materials. Bulk modulus and shear modulus of the tough hydrogel [22, S2] was 2.21 GPa and 10.8 KPa, respectively and the acoustic velocity and density of water were 1466 m/s and 1000 kg/m^3, respectively (See Supporting Text). The air was considered to be non-dissipative, the acoustic velocity and density of which are assumed to be 343 m/s and 1.204 kg/m^3, respectively. The density and velocity of the liquid metal are taken as 6250 kg/m^3 and 2847 m/s, respectively [S1]. Quadratic serendipity and quadratic Lagrange elements were used for solid and acoustic materials, respectively, with the largest element size smaller than one tenth of acoustic wavelength. The right and left ends of the meta-gel unit cell were set as periodic boundary condition, and all the interfaces between hydrogel and fluid (air and water) were set to be Acoustic-Structure Boundaries. The top and bottom sides of the simulation region were surrounded by perfectly matched layer (PML). Background pressure field was applied in the whole model to provide an incident sound pressure. Two integral regions were defined to obtain the transmission coefficient and reflection coefficient corresponding to each order. The jth order transmission coefficient and reflection coefficient were evaluated by

$$T_j = \int p_t \exp(ik_{jx}x + ik_{jy}y)ds / S_{region1} \quad \text{and} \quad R_j = \int p_s \exp(ik_{jx}x - ik_{jy}y)ds / S_{region2},$$ respectively, where p_t was the total acoustic pressure, p_s was the scattered acoustic pressure, S was the area of the integral region, $k_{jx} = 2\pi/(a * j)$ and $k_{jy} = sqrt(k_0^2 - k_{jx}^2)$ were wave vector components of the jth order diffracted plane wave (a was the width of the model and k_0 was the incident wave number). The total energy transmission coefficient and reflection coefficient were expressed as $TE = b_j T_j^2$ and $RE = b_j R_j^2$, where b_j was the ratio between k_{jy} and k_0.
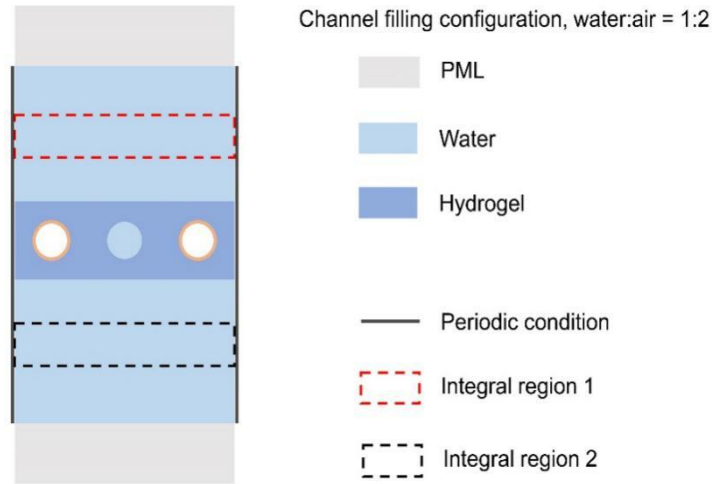
Figure S4. Simulation model in COMSOL based on the multiple scattering decomposition method.

Acoustic transmission coefficient of meta-gel sheet using MST model and COMSOl simulation

Using MST and COMSOL simulation, we calculate the acoustic transmission coefficient over a wide frequency range of 0.4 KHz to 5 MHz (**Figure S5**) for the sample with dimensions a=2.2 mm and L=6.5 mm. MST and COMSOL simulation matches very well. According to the calculation, when the channels are filled with water, the transmission coefficient of meta-gel still maintains almost 1 from 0.4 KHz to 5 MHz, which also has been proved by experimental test and previous work [22]. By change the filling ratio N_{air} and N_{water}, transmission coefficient in the range from 0 to 1 can be achieved from 0.4 KHz to 150 KHz, beyond the range in experimental measurements. In addition, as increasing frequency range, acoustic transmission coefficient of the meta-gel gradually approaches to almost constant over MHz. Besides the MST model, the wave transmission behavior in this high frequency range can also be explained by the principle of geometrical acoustics [S1]. The number of acoustic rays transmitted through the meta-gel layer is proportional to the projected area of the meta-gel regions that are impedance matched with water (i.e., the hydrogel part) on a plane

10

perpendicular to the acoustic rays. The lowest acoustic transmission coefficient of air-gel sheet that can be achieved by the currently fabricated meta-gel sample with a=2.2 mm and L=6.5 mm is around 0.68. The area fraction of air-to-water for the fabricated meta-gel is 2.2:4.3. The acoustic transmission through the meta-gel is 4.3/(2.2+4.3)=0.66, which matches with the MST model and numerical simulation. The transmission coefficient increases linearly with the increase of L (i.e., the decrease of air's volume fraction). Thus, tunable transmission coefficient fully covering the range from 0 to 1 in high frequency can be achieved by designing air's volume fraction.
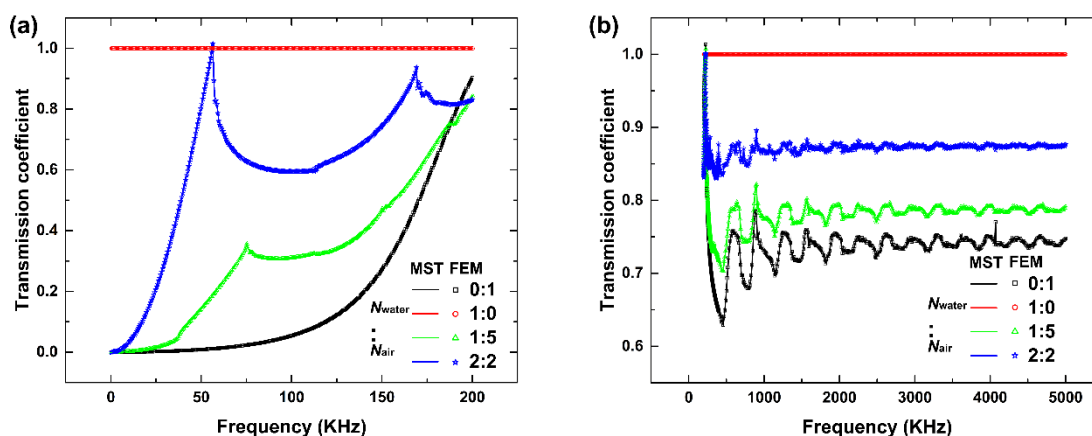

Figure S5. Transmission coefficient of the meta-gel in frequency range 0.4 KHz to 5 MHz. The filling ratio N_{water} and N_{air} is 0:1, 1:5, 2:2 and 1:0, respectively. The width of the channel in the meta-gel is 2.2 mm and the distance between two adjacent channels is 6.5 mm.

Acoustic impedance of meta-gel and other composites calculated by effective parameter retrieving method

When the wavelengths of acoustic waves in water are larger than the feature sizes of our current design of meta-gel sheet, we can approximate the meta-gel sheet as a macroscopically homogeneous

material. We calculate the effective acoustic impedance of meta-gel using combination of numerical simulation and the effective parameter retrieval method [S2]. The meta-gel sheet with different channel dimensions was first investigated by using the Acoustic-Solid Interaction Module in COMSOL Multiphysics. A periodic super cell of meta-gel composites was placed in a 2D waveguide. Periodic boundary condition was set to the left and right boundaries of the super cell. A plane wave in designed frequency range was incident to the meta-gel sheet filled with water and the reflection field R_0 and transmission field T_0 were recorded. The R_0 and T_0 can also be obtained by MST model according to **Eq. S9**. The acoustic impedance of the material was then calculated as

$Z = \pm \sqrt{\dfrac{(1+R_0)^2 - T_0^2}{(1-R_0)^2 - T_0^2}} Z_{water}$, following the effective parameter retrieving method [S2], where Z_{water} is

the acoustic impedance of the water (**Table S1**). The sign was determined by requiring that the real part of the impedance be positive. The real part of the Z was compared with acoustic impedance of other materials. During the calculation, the thickness of the meta-gel layer is set to be identical to the diameter of the channel. The other pure hydrogel part is neglected since the acoustic properties of hydrogel was identical to that of water. Normalized impedance is defined as the ratio of acoustic impedance of meta-gel to that of water. The acoustic impedance of water is $1466 \ 10^3$ Pa s m^{-1}. Normalized impedances for different channel dimensions and filling materials are plotted in Figure S6.

The densities and sound velocities of different materials including solid, liquid and gas were listed on **Table S1-3** below. The acoustic impedances of the materials were then calculated as the product of the density and sound velocity.
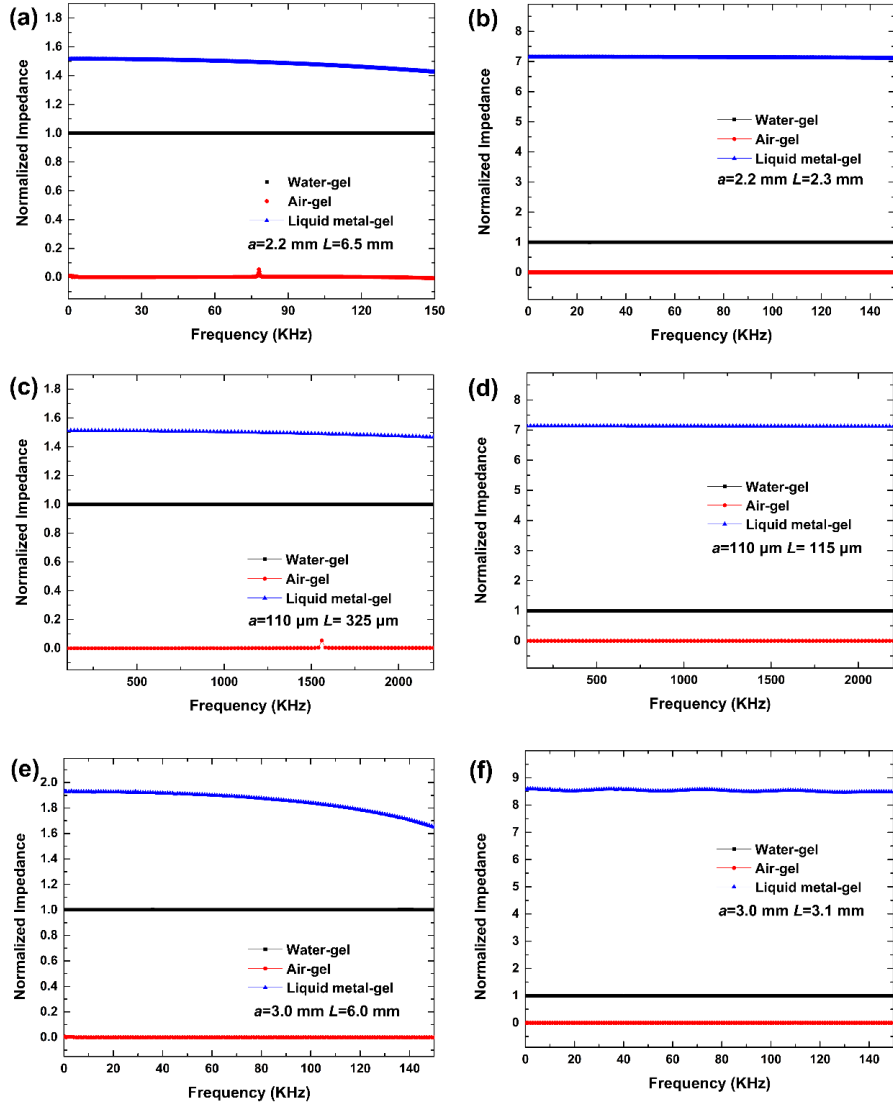
Figure S6. Normalized impedance (Z/Z_water) of different meta-gel sheets filled by water, air and liquid metal. The acoustic impedance of water is 1466×10^3 Pa s m^{-1}.

13

Table S1. Acoustic properties of solid [S3]

Material	Density (Kg m^{-3})	Acoustic impedance (Pa s m^{-1} 10^3)
Fiberglass	1500	4110
Lucite	1180	3162
Nylon	1120	2912
Polyethylene	910	1892.8
Polystyrene	1030	2410
Acrylic (Perspex)	1190	3249
Polyvinylchloride, (PVC)	1390	3329
Silicone rubber	1100	1634
Wood	1000	3300~5000
Brick	1400~2400	5040~10080
Concrete	2400	7680~8880
Granite	1800~2600	10710~15470
Glass, Pyrex	1400~1800	7896~10152
Glass, Pyrex	1800	10152
bone	1912	7801
fat	952	1389
muscle	1080	1706
blood	1057	1665

Table S2. Acoustic properties of liquid [S3]

Material	Density (Kg m^{-3})	Acoustic impedance (Pa s m^{-1} 10^3)
Acetone	785	850
Benzene	874	958
Carbon Tetrachloride	1584	1446
Ethyl Alcohol	789	915
Gasoline	711	961
Gasoline	737	979
Glycerin	1259	2340
n-Hexanol	811	1057
Kerosene	820	1033
Motor oil	880	1531
Motor	940	1636
Petrol	711	872
Petrol	737	888
Petrol	711	1029
Petrol	737	1048
Octane	692	810
Oil (castor)	956	1425
Oil (lubricating)	900	1315
Phenol	956	1218
n-Propanol	804	970
Pyridine	979	1387
Toluene	867	1132
Turpentine	870	1079
Water	1000	1466
Sulfuric Acid	1838	2349
Seawater	1025	1549

Table S3. Acoustic properties of gas [S3]

Material	Density (Kg m^{-3})	Impedance (10^3 Pa s m^{-1})
Acetylene	1.092	0.359
Air	1.204	0.413
Ammonia (30°C)	0.717	0.315
Argon	1.661	0.511
Carbon monoxide	1.165	0.391
Chloroform (22°C)	2.994	0.461
Ethane	1.264	0.399
Ethylene (20°C)	1.26	0.412
Helium	0.1664	0.162
Hydrogen	0.0899	0.116
Hydrogen chloride	1.528	0.453
Hydrogen sulfide (24°C)	1.434	0.443
Neon (30°C)	0.899	0.4144
Nitric oxide (16°C)	1.249	0.4172
Nitrogen (29°C)	1.165	0.4129
Oxygen	1.331	0.4206

SReferences

[1] C. M. Linton, P. McIver, *Handbook of Mathematical Techniques for Wave/Structure Interactions*, CRC Press, Boca Raton, **2001**.

[2] T. Zhang, S. Lin, H. Yuk, X. Zhao, *Extreme Mech. Lett.* **2015**, *4*, 1.

[3] Engineering ToolBox, https://www.engineeringtoolbox.com/, accessed: 3, **2019**.